Supporting Information

The SALSAC Approach: Comparing the reactivity of solvent-dispersed nanoparticles with nanoparticulate surfaces

Sven A. Freimann,[a] Davood Zare,[a] Catherine E. Housecroft[a] and Edwin C. Constable*[a]

[a] Department of Chemistry, University of Basel, BPR 1096, Mattenstrasse 24a, CH-4058 Basel, Switzerland.
email: edwin.constable@unibas.ch

Experimental Details of Instruments

^{1}H NMR, ^{13}C{^{1}H} NMR and ^{31}P{^{1}H} NMR spectra were measured at 298 K on a Bruker Avance III-500 NMR spectrometer. ^{1}H, ^{13}C and ^{31}P chemical shifts were referenced to residual solvent peaks with respect to δ(TMS) = 0 ppm for ^{1}H and ^{13}C{^{1}H} and δ(H_3PO_4 85% aqueous) = 0 ppm for ^{31}P{^{1}H}. A Gaussian fit to the diffusion peak intensity was done to determine the diffusion constant of the signal. The PFGSE experiments were performed using a bipolar gradient pulse sequence.[1] The sigmoidal intensity decrease was fitted with a two-parameter fit (I_0 and diffusion coefficient D) with the DOSY routine implemented in topspin 4.0 [Bruker Biospin GmbH, 2016].

Reactions under microwave conditions were carried out in a Biotage Initiator 8 reactor. An Eppendorf Centrifuge 5415 R was used for 2 mL samples while a Hettich Centrifuge Universal 320 was used for 10 mL samples.

Solution absorption spectra were recorded on an Agilent Cary 5000 spectrophotometer and for solid-state absorption spectra, a Diffuse Reflectance Accessories was added to the spectrophotometer. For each solid-state absorption spectrum, a baseline correction was done with the respective nanoparticle precursor. Infrared spectra were recorded on a Perkin Elmer UATR Two spectrometer. Electrospray ionization (ESI) mass spectra and high resolution ESI MS were measured on a Shimadzu LCMS-2020 or a Bruker maXis 4G instrument, respectively.

Scanning electron microscopy (SEM) was performed using an Hitachi S-4800 instrument with an acceleration voltage of 5 kV and a working distance of 4 mm. Particle sizes were measured with a nanoimaging tool from the Nano Imaging Lab, University of Basel.

Thermogravimetric analysis (TGA) was performed on a TGA/SDTA851 (Mettler Toledo) instrument under nitrogen. Initially, the temperature was held at 30 °C for 10 min before heating at a rate of 10 °C/min to 120 °C. This temperature was maintained for 30 min to remove all traces of water. Afterwards the sample was heated to 900 °C at a rate of 10 °C/min. After maintaining the temperature at 900 °C for 30 min, the sample was cooled to ambient temperature.

---

[1] D.H. Wu, A.D. Chen and C.S.J. Johnson, *Magn. Reson. A*, 1995, **115**, 260-264.

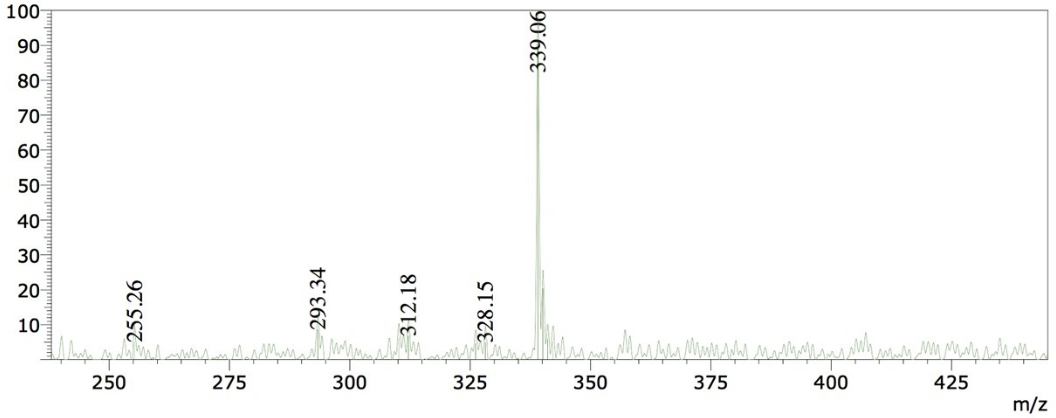

Fig. S1. Electrospray mass spectrum of **2** (with aqueous NH_3, negative mode).

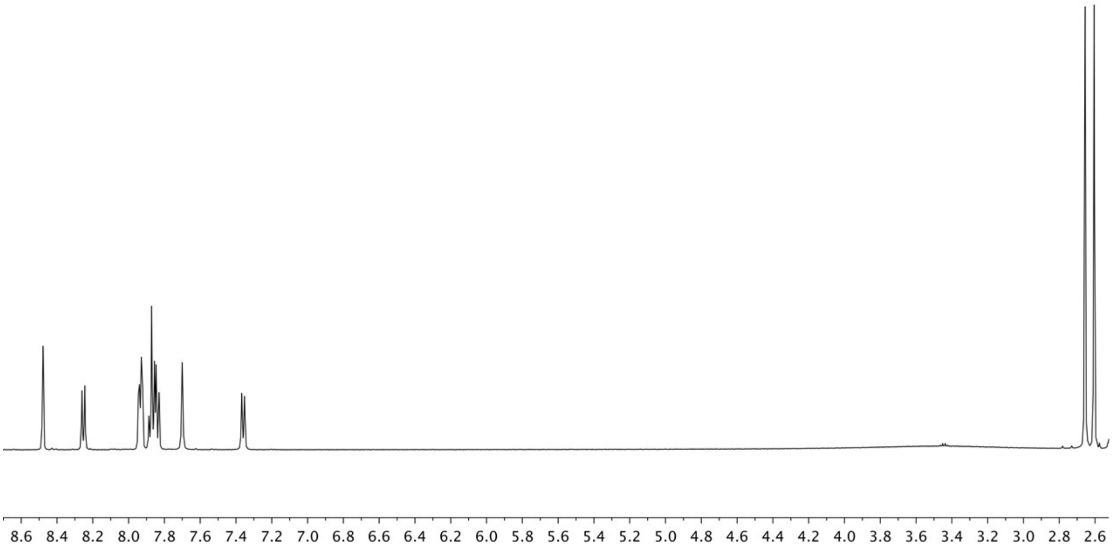

Fig. S2. ^1H NMR (500 MHz, DMSO-d_6, 298 K) spectrum of compound **2**. δ / ppm.

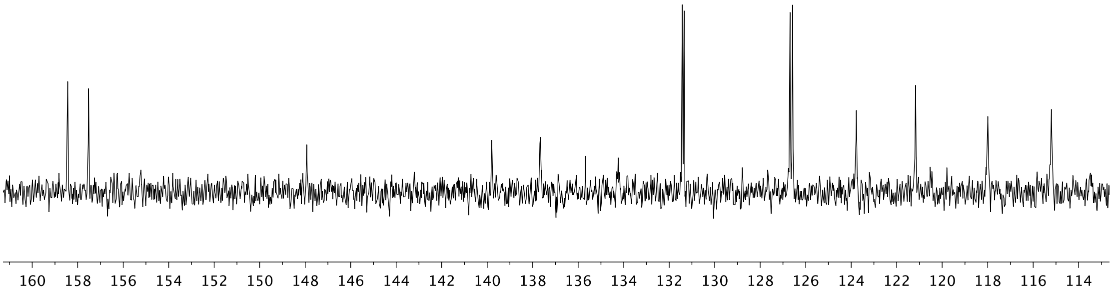

Fig. S3. $^{13}C\{^1H\}$ NMR (126 MHz, DMSO-d_6, 298 K) spectrum (aromatic region) of compound **2**. δ / ppm.

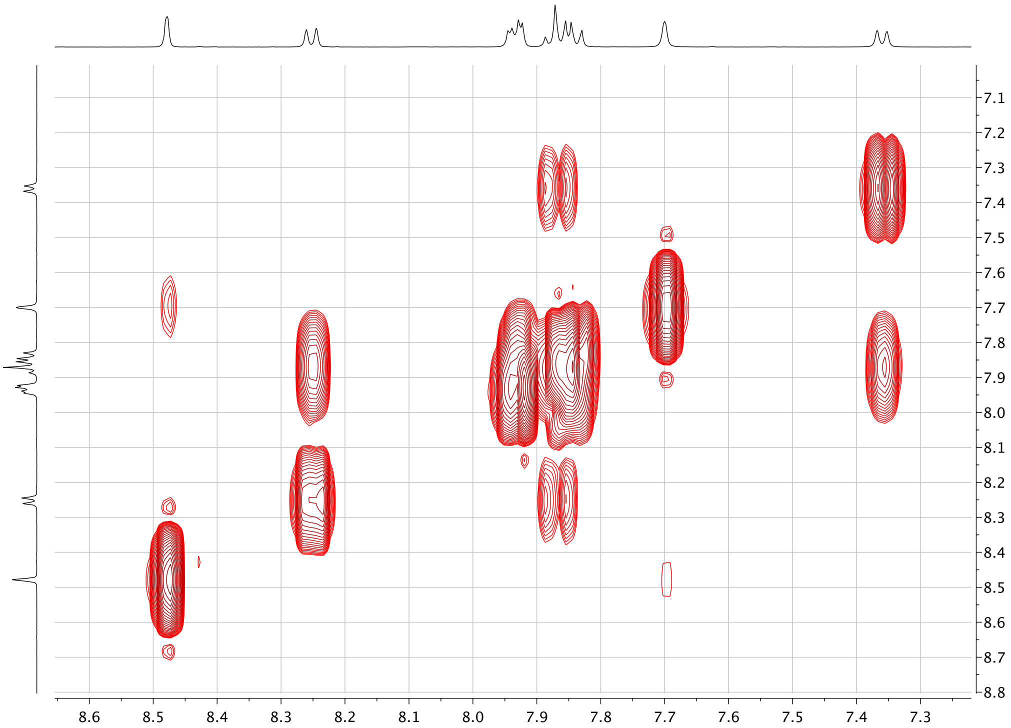

Fig. S4. COSY (500 MHz, DMSO-d_6, 298 K) spectrum of compound **2**. δ / ppm.

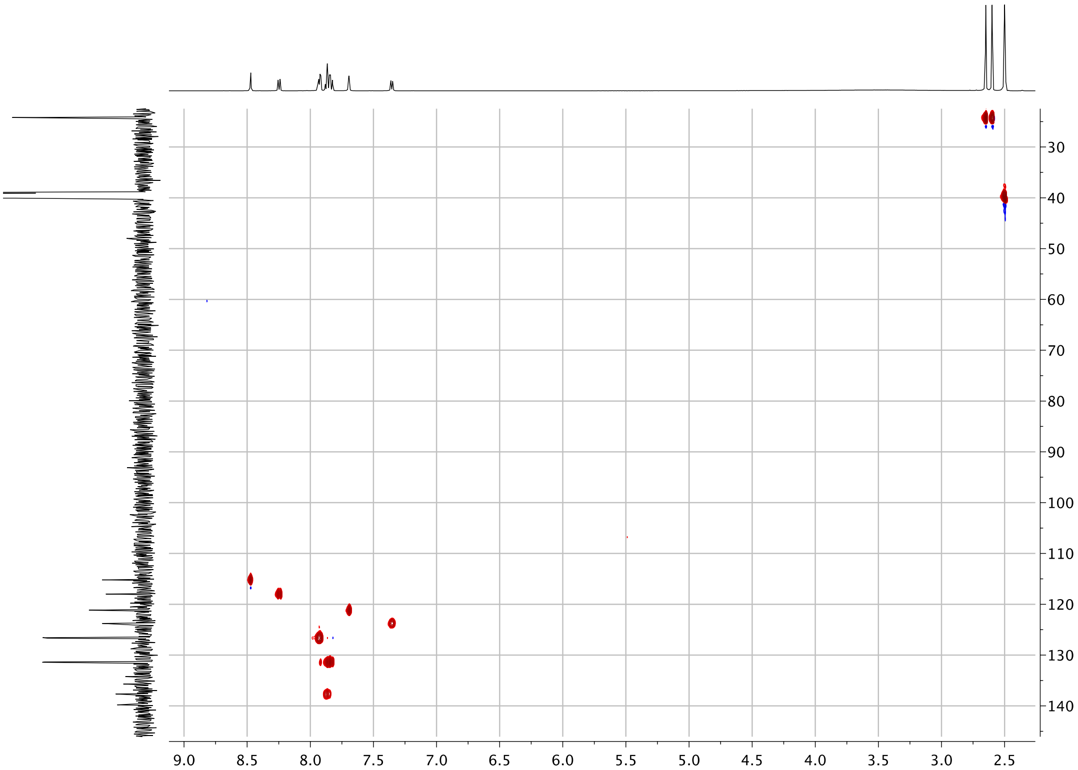

Fig. S5. HMQC (500 MHz ^{1}H, 126 MHz ^{13}C, DMSO-d_6, 298 K) spectrum of compound **2**. δ / ppm.

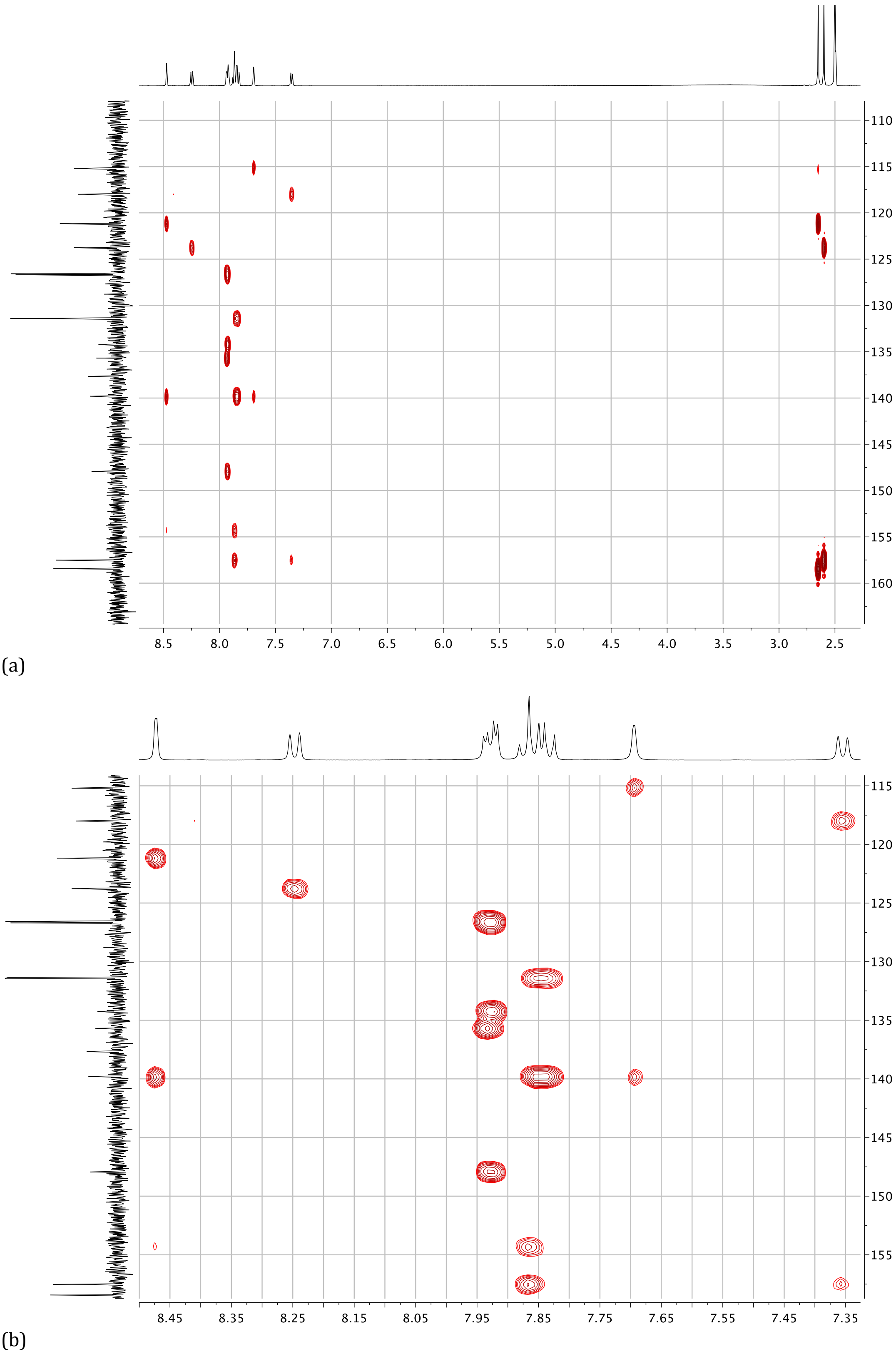

Fig. S6. (a) HMBC (500 MHz ^{1}H, 126 MHz ^{13}C, DMSO-d$_6$, 298 K) spectrum of compound **2**, and (b) an expansion of the aromatic region. δ / ppm.

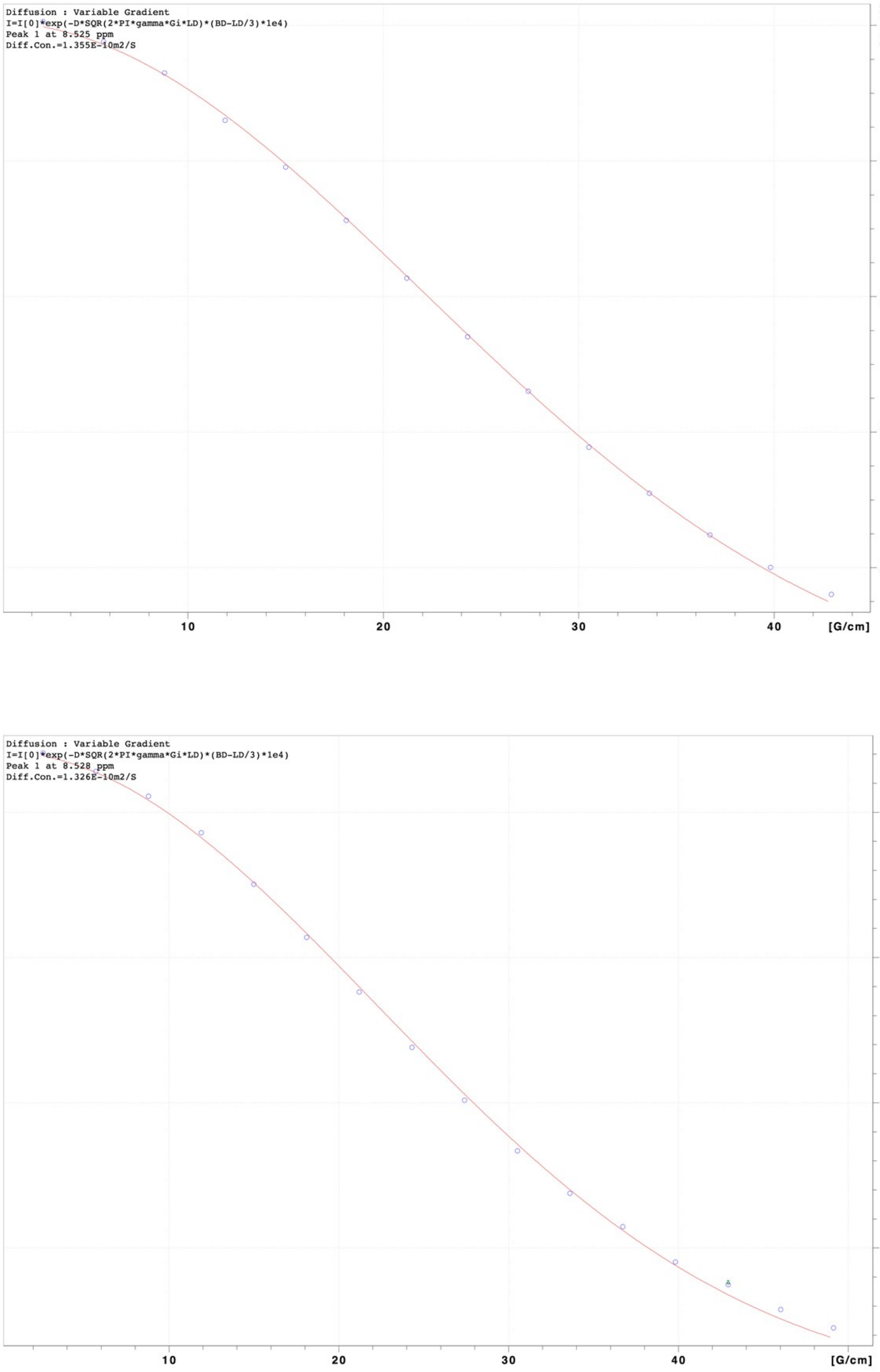

(a)

(b)

Fig. S7. Fits to the DOSY intensities for (a) ligand **1** in DMSO-d_6, and (b) a DMSO-d_6 solution containing dispersed NPs which had been treated with **1** following Procedure A in the Experimental Section.

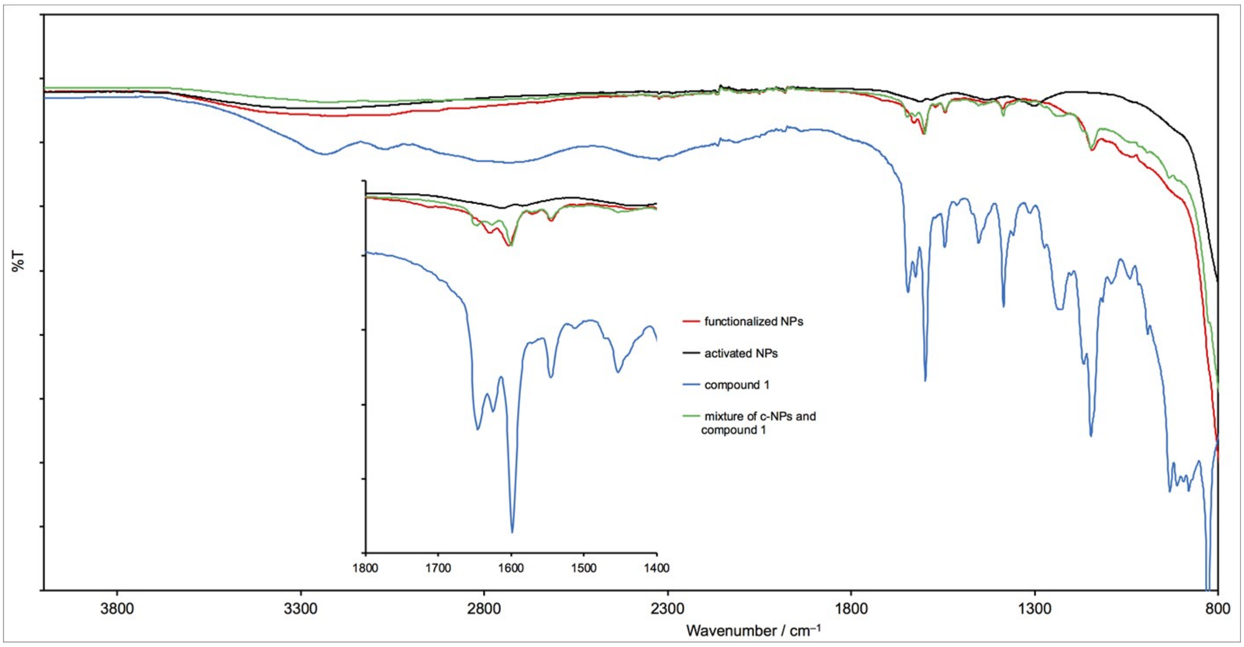

Fig. S8. Solid-state IR spectra of activated NPs (a-NPs), pristine **1**, a-NPs functionalized with **1** following Procedure B in the Experimental Section, and a mixture of commercial NPs (c-NPs) and **1**.

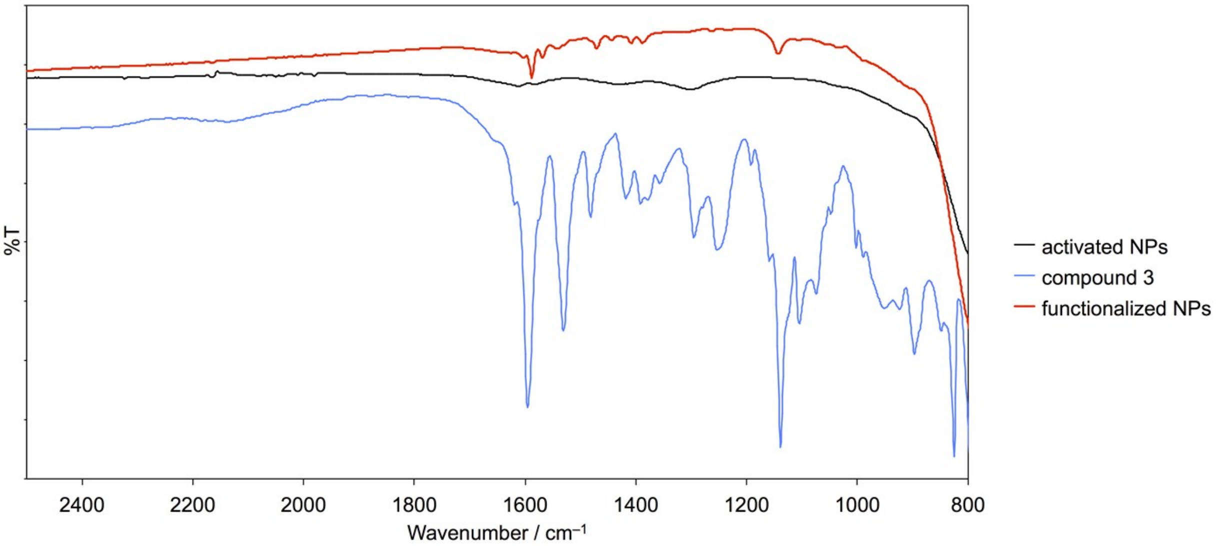

Fig. S9. Solid-state IR spectra of activated NPs, pristine **3**, and NPs functionalized with **3** following the Procedure B in the Experimental Section.

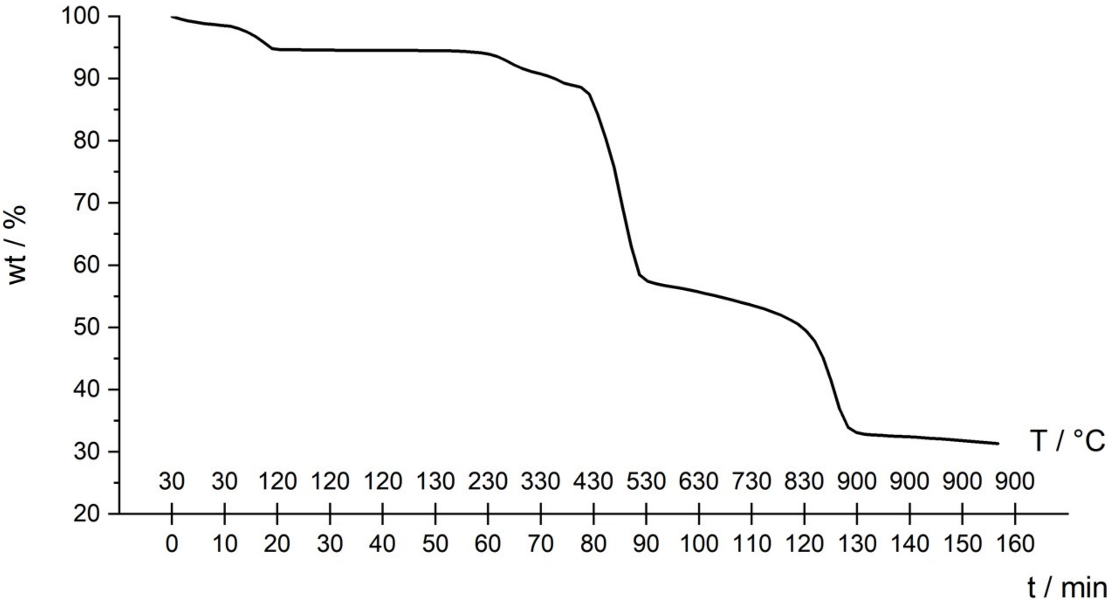

Fig. S10. TGA curve for ligand **1**.

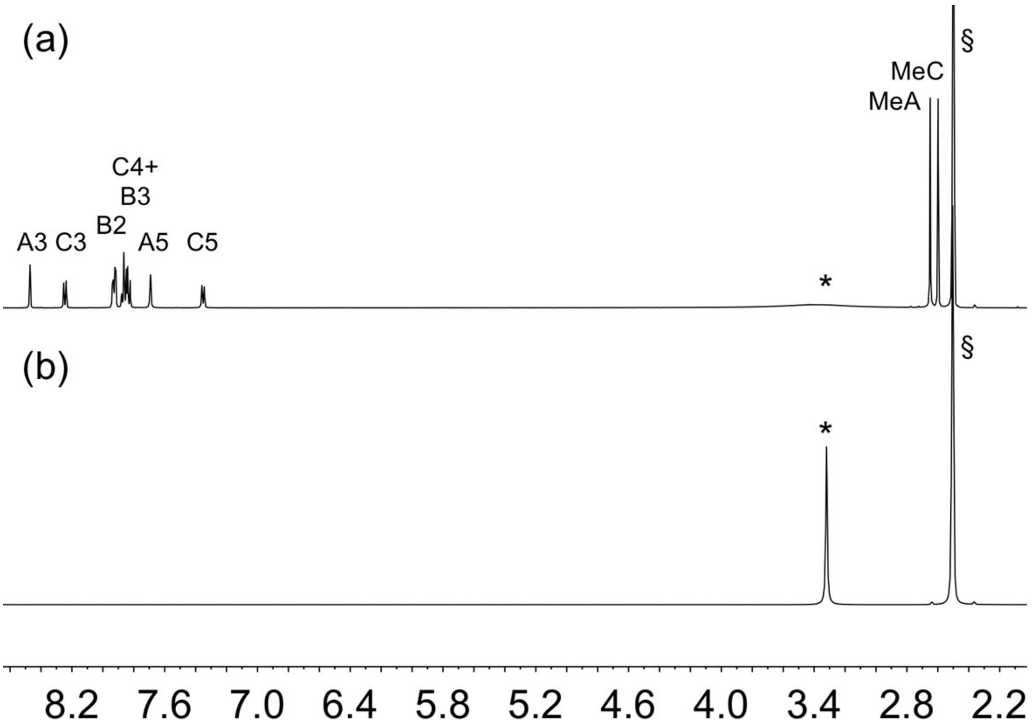

Fig. S11. ^{1}H NMR (500 MHz, DMSO-d_6, 298 K) of (a) ligand **2** and (b) suspended residue after activated TiO_2 NPs had been functionalized with **2** following Procedure B in the Experimental Section. See Scheme 1 for atom labelling. Chemical shifts in δ / ppm. § = residual DMSO-d_5. * = water.

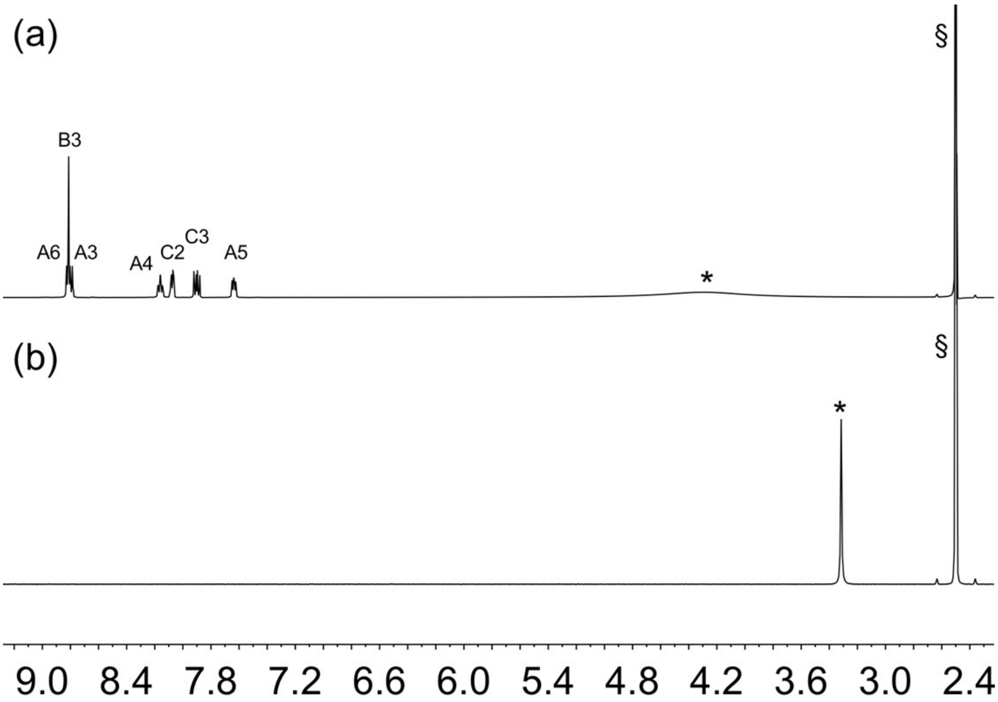

Fig. S12. ^{1}H NMR (500 MHz, DMSO-d_6, 298 K) of (a) ligand **3** and (b) suspended residue after activated TiO_2 NPs had been functionalized with **3** following Procedure B in the Experimental Section.. See Scheme 1 for atom labelling. Chemical shifts in δ / ppm. § = residual DMSO-d_5. * = water.

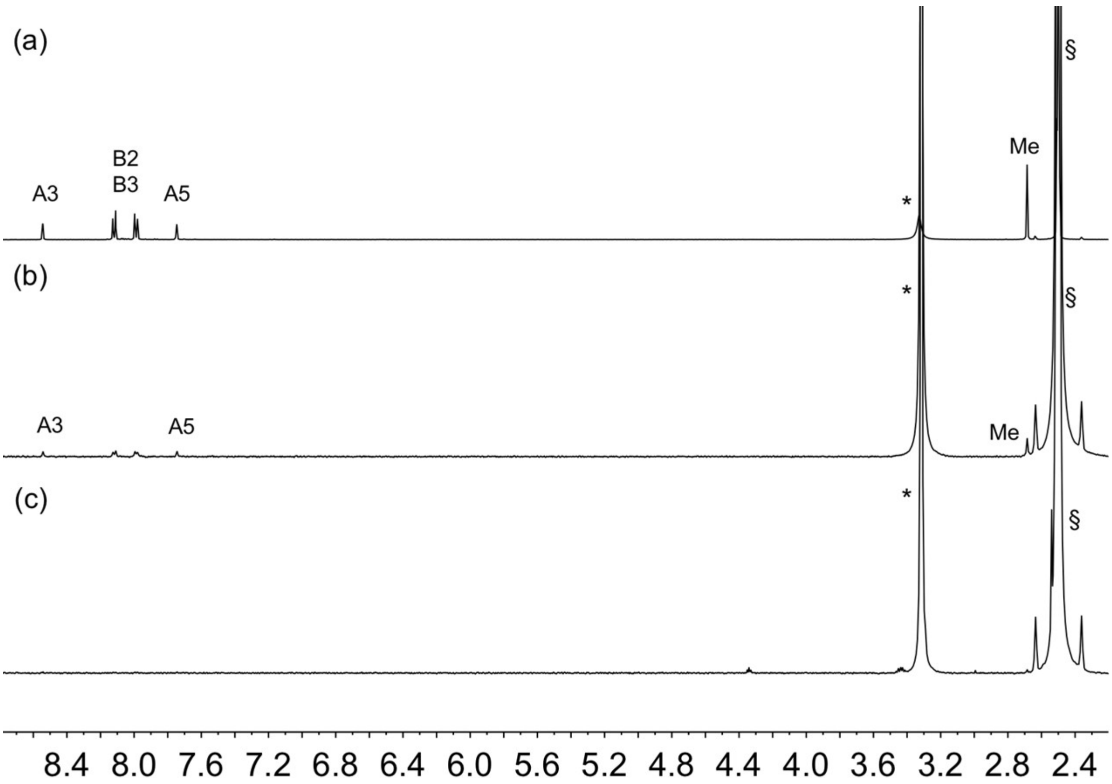

(b) expansion

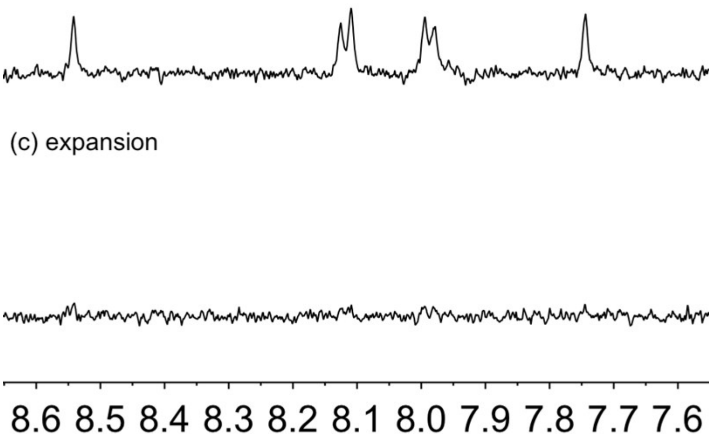

Fig. S13. ^{1}H NMR (500 MHz, DMSO-d_6, 298 K) of (a) ligand **4**, (b) suspended residue after activated TiO_2 NPs had been functionalized with **4** following Procedure B in the Experimental Section, and (c) the same residue after washing with DMSO and EtOH. Expansions of the aromatic region in (b) and (c) are also shown. See Scheme 1 for atom labelling. Chemical shifts in δ / ppm. § = residual DMSO-d_5. * = water.

(a) (b)

Fig. S14 Photographs of activated TiO_2 NPs functionalized (a) with **2** and after treatment with $[Cu(MeCN)_4][PF_6]$, and (b) with **4** and after treatment with $[Cu(MeCN)_4][PF_6]$.

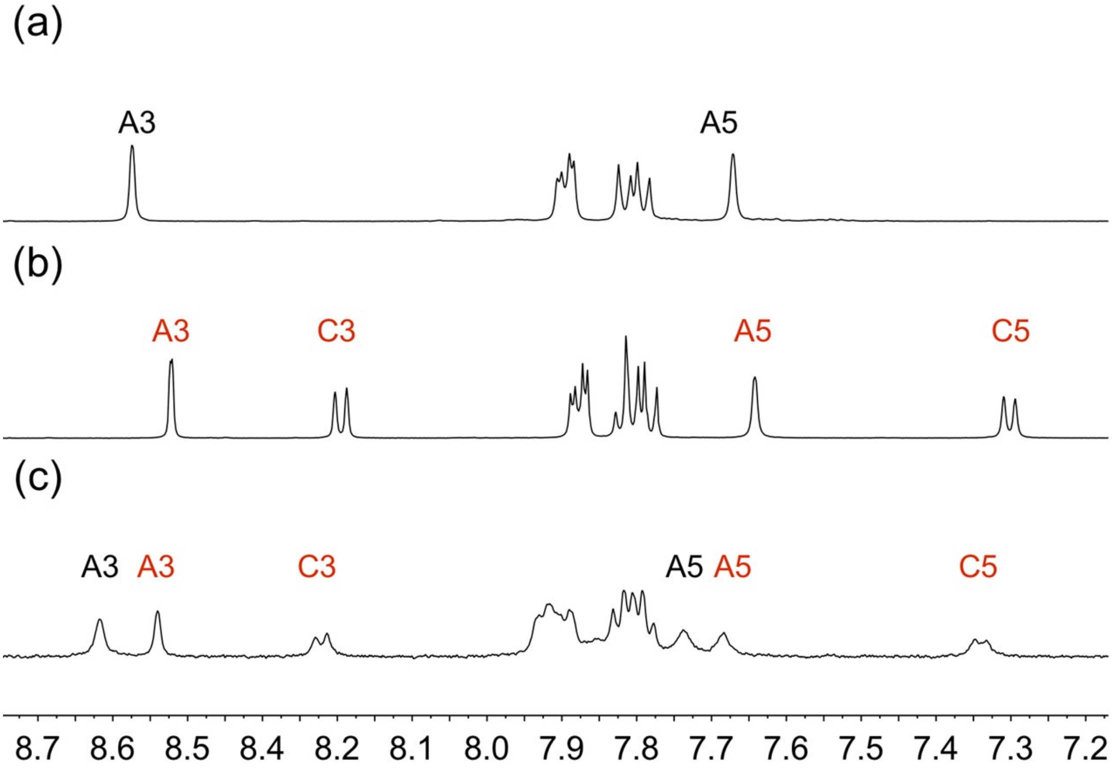

Fig. S15. ^1H NMR (500 MHz, DMSO-d_6, 298 K) of (a) ligand **1**, (b) ligand **2**, (c) suspended residue after activated TiO_2 NPs had been functionalized with a 1:1 mixture of **1** and **2** following Procedure C in the Experimental Section. See Scheme 1 for atom labelling. Chemical shifts in δ / ppm.

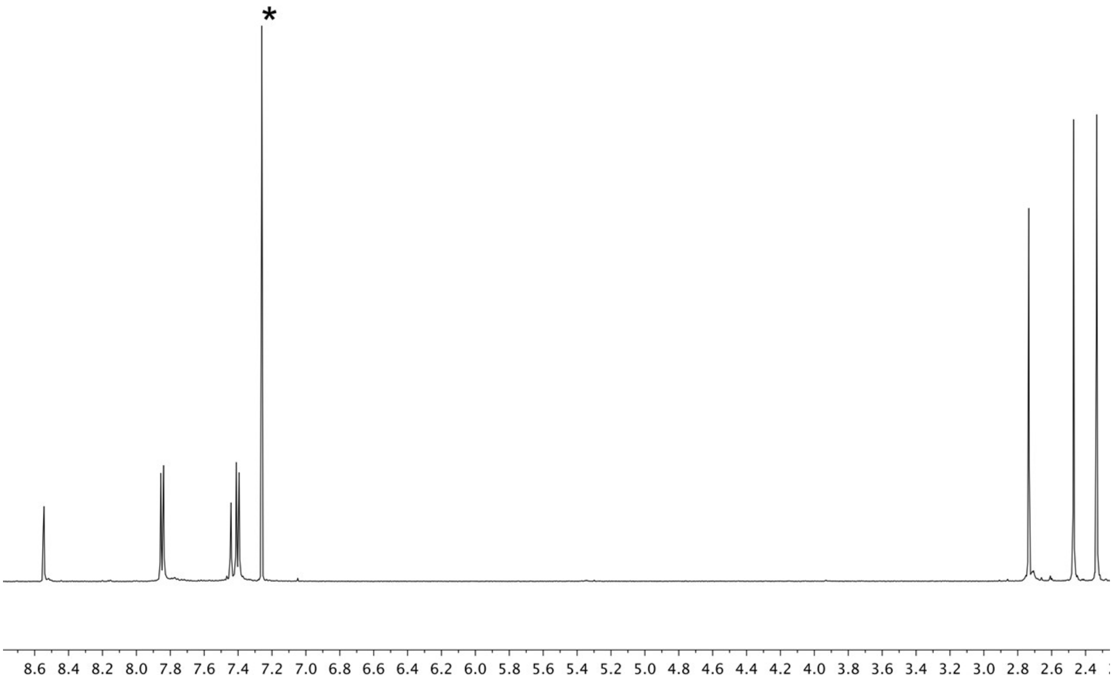

Fig. S16. ^{1}H NMR (500 MHz, $CDCl_3$, 298 K) spectrum of compound **7**. * = residual $CHCl_3$. δ / ppm.

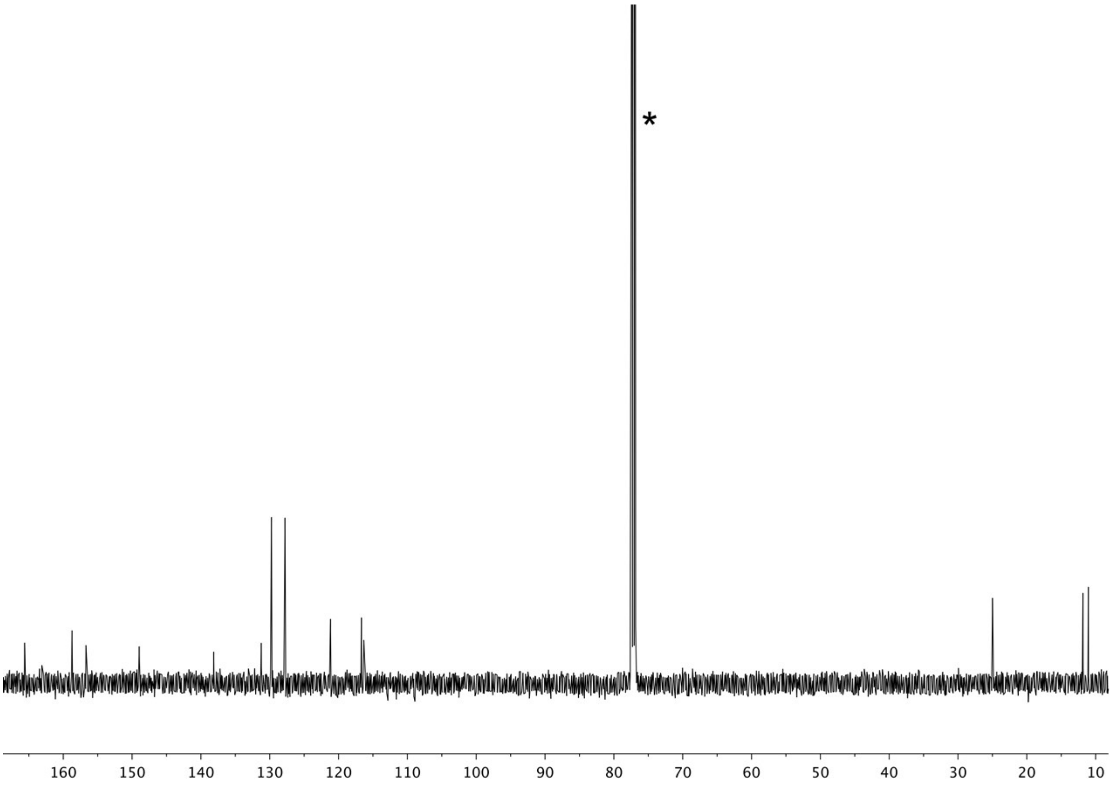

Fig. S17. $^{13}C\{^1H\}$ NMR (126 MHz, $CDCl_3$, 298 K) spectrum of compound **7**. * = $CDCl_3$. δ / ppm.

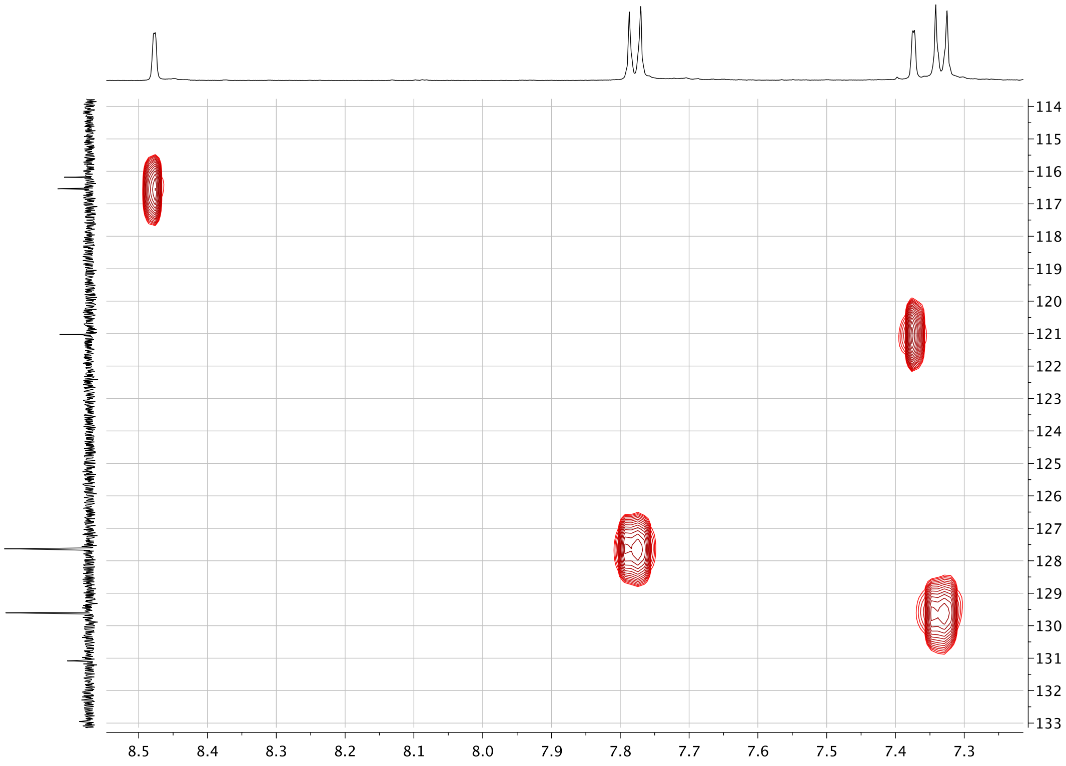

(a)

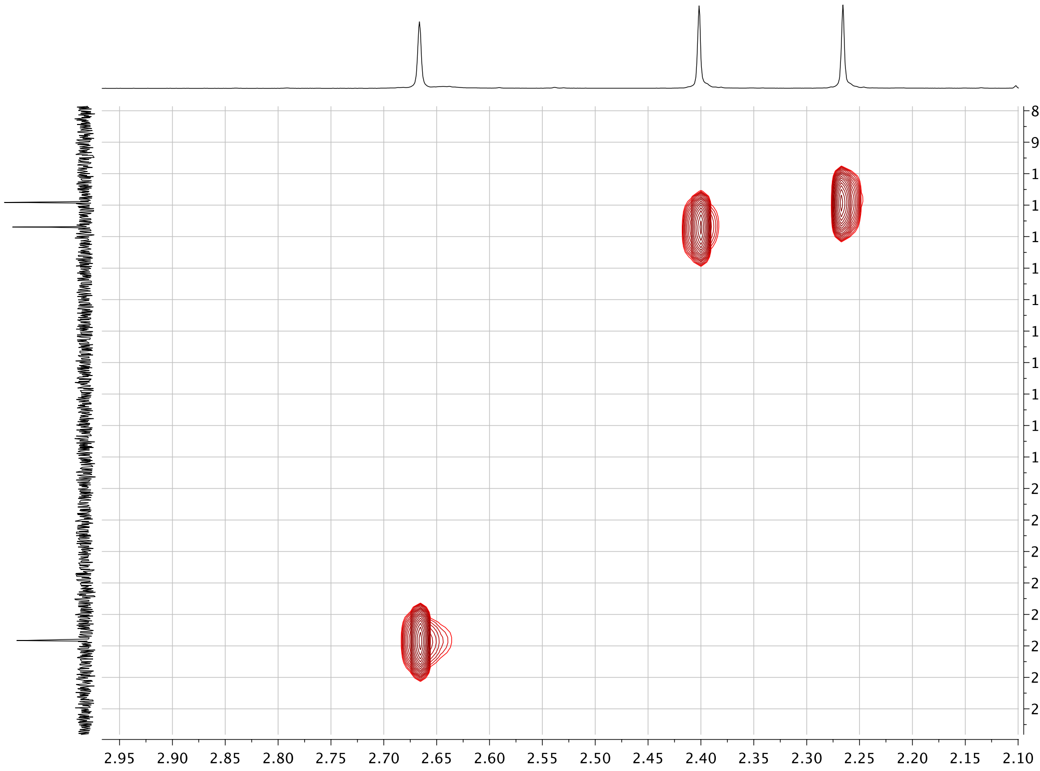

(b)

Fig. S18. HMQC (500 MHz ^{1}H, 126 MHz ^{13}C, CDCl$_3$, 298 K) spectrum of compound **7**: (a) aromatic region, (b) methyl signals. δ / ppm.

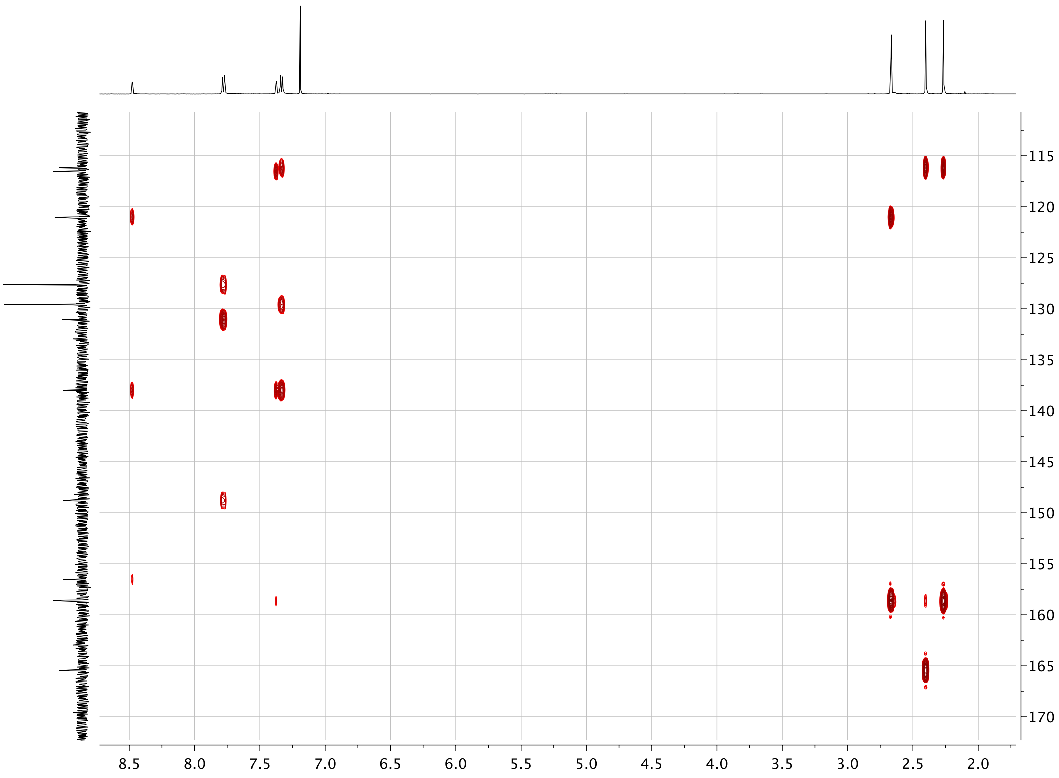

Fig. S19. HMBC (500 MHz ^{1}H, 126 MHz ^{13}C, CDCl$_3$, 298 K) spectrum of compound **7**. *δ* / ppm.

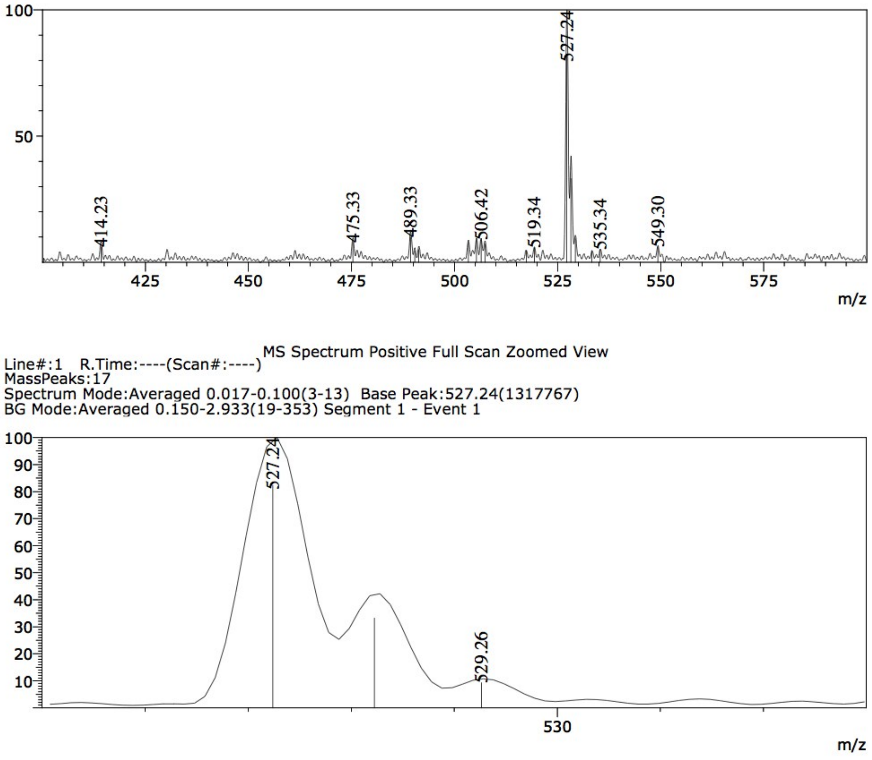
```
Line#:1   R.Time:----(Scan#:----)
MassPeaks:17
Spectrum Mode:Averaged 0.017-0.100(3-13)  Base Peak:527.24(1317767)
BG Mode:Averaged 0.150-2.933(19-353) Segment 1 - Event 1
```

Fig. S20. Electrospray mass spectrum of **7** (with formic acid, positive mode).

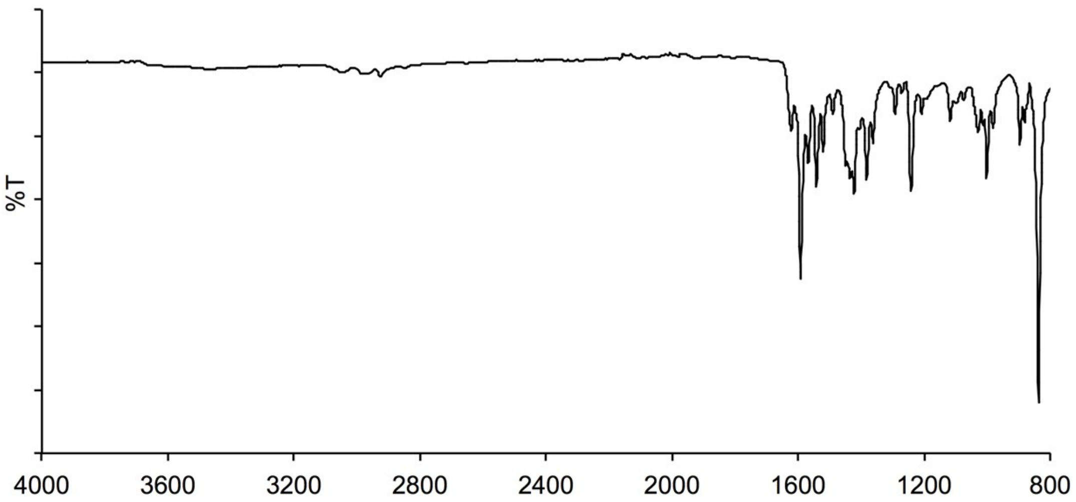

Fig. S21. FT-IR spectrum of solid **7**.

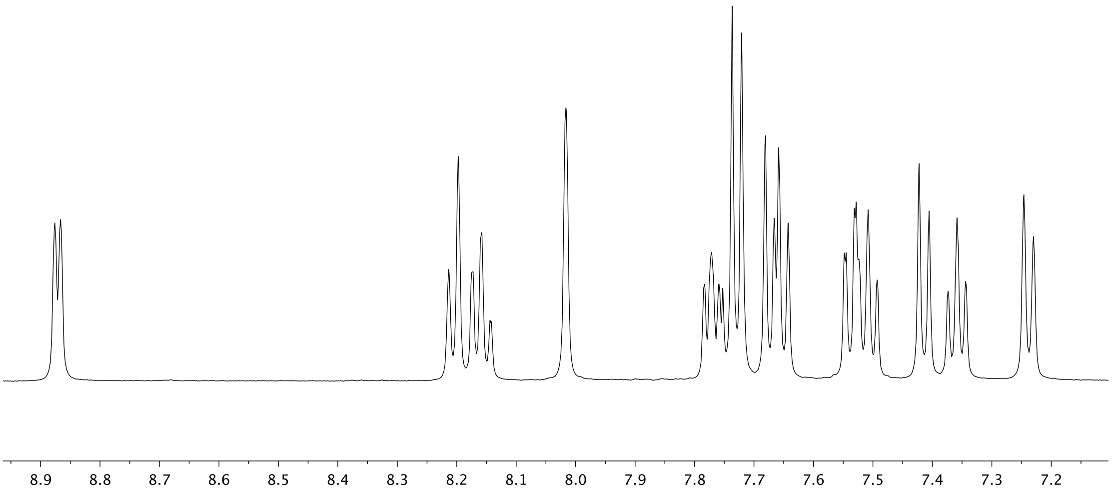

Fig. S22. ^{1}H NMR (500 MHz, acetone-d_6, 298 K) spectrum (aromatic region) of $[Cu(\mathbf{6})_2][PF_6]$. δ / ppm.

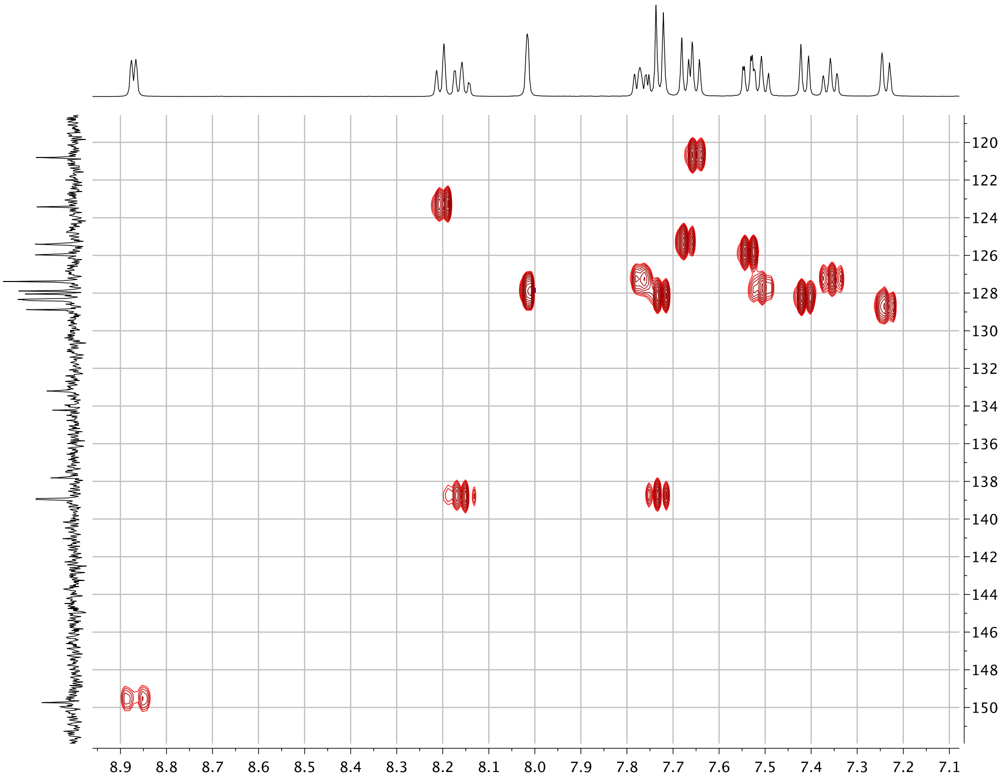

Fig. S23. HMQC (500 MHz ^{1}H, 126 MHz ^{13}C, acetone-d$_6$, 298 K) spectrum of [Cu(**6**)$_2$][PF$_6$]. δ / ppm.

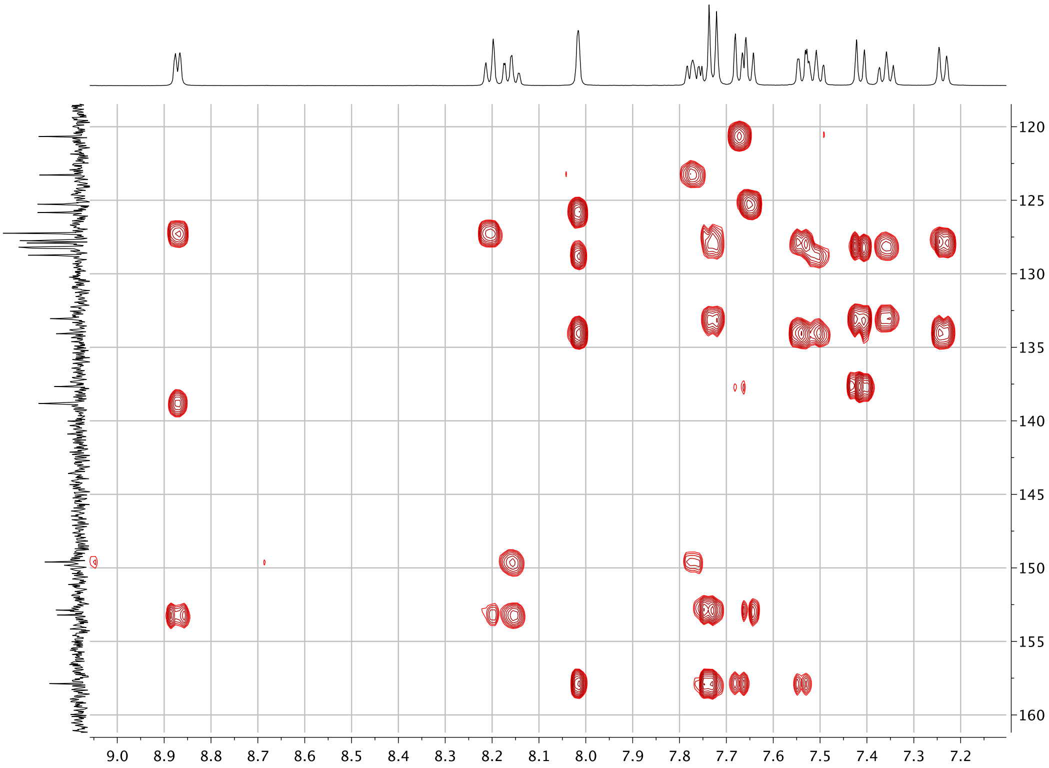

Fig. S24. HMBC (500 MHz ^{1}H, 126 MHz ^{13}C, acetone-d$_6$, 298 K) spectrum of [Cu(**6**)$_2$][PF$_6$]. δ / ppm.

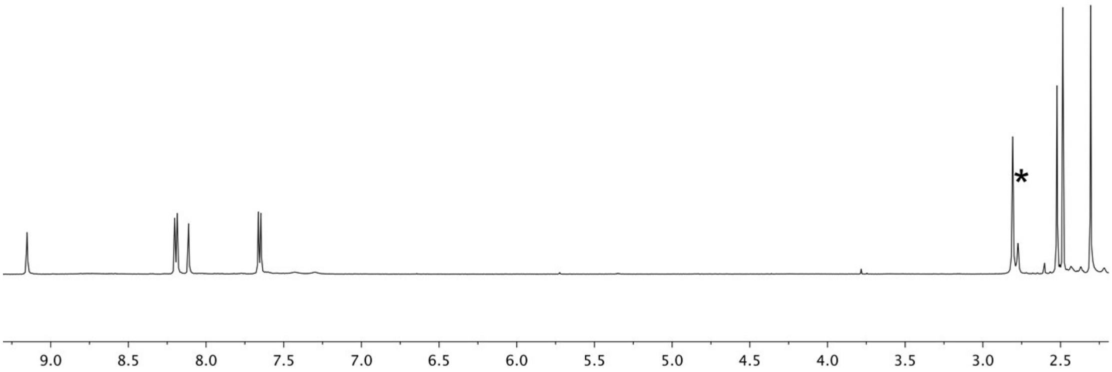

Fig. S25. ^{1}H NMR (500 MHz, acetone-d$_6$, 298 K) spectrum of [Cu(**7**)$_2$][PF$_6$]. * = H_2O, HOD. δ / ppm.

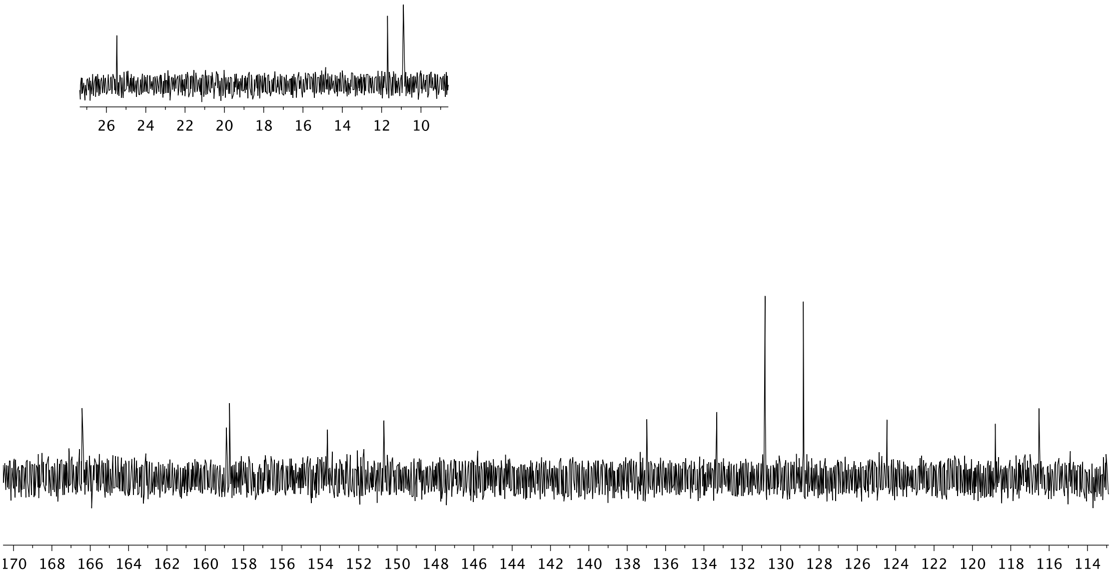

Fig. S26. ^{13}C{^{1}H} NMR (126 MHz, acetone-d$_6$, 298 K) spectrum of [Cu(**7**)$_2$][PF$_6$], aromatic region with methyl region inset. δ / ppm

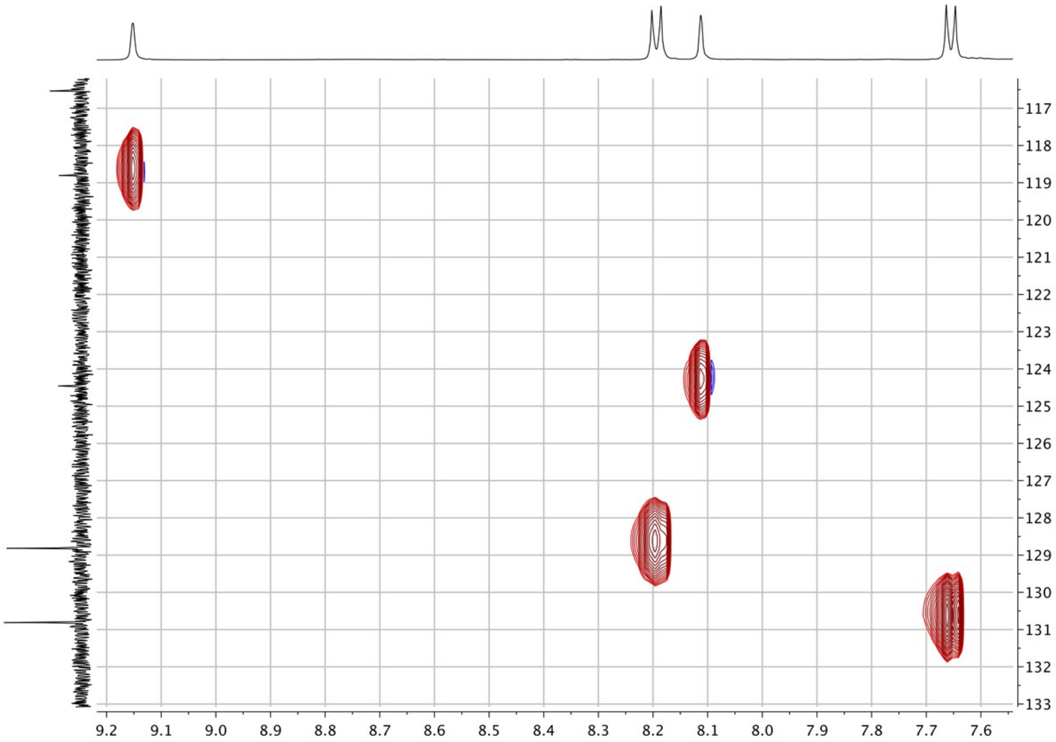

(a)

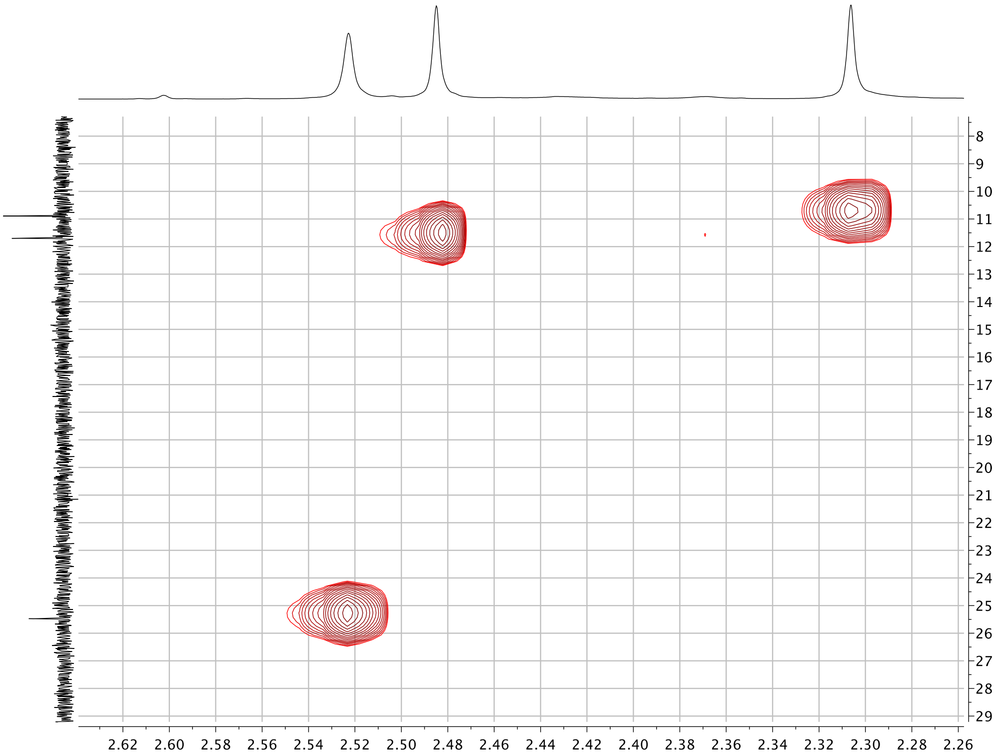

(b)

Fig. S27. HMQC (500 MHz ^{1}H, 126 MHz ^{13}C, acetone-d_6, 298 K) spectrum of [Cu(**7**)$_2$][PF$_6$]: (a) aromatic region, (b) methyl signals. δ / ppm.

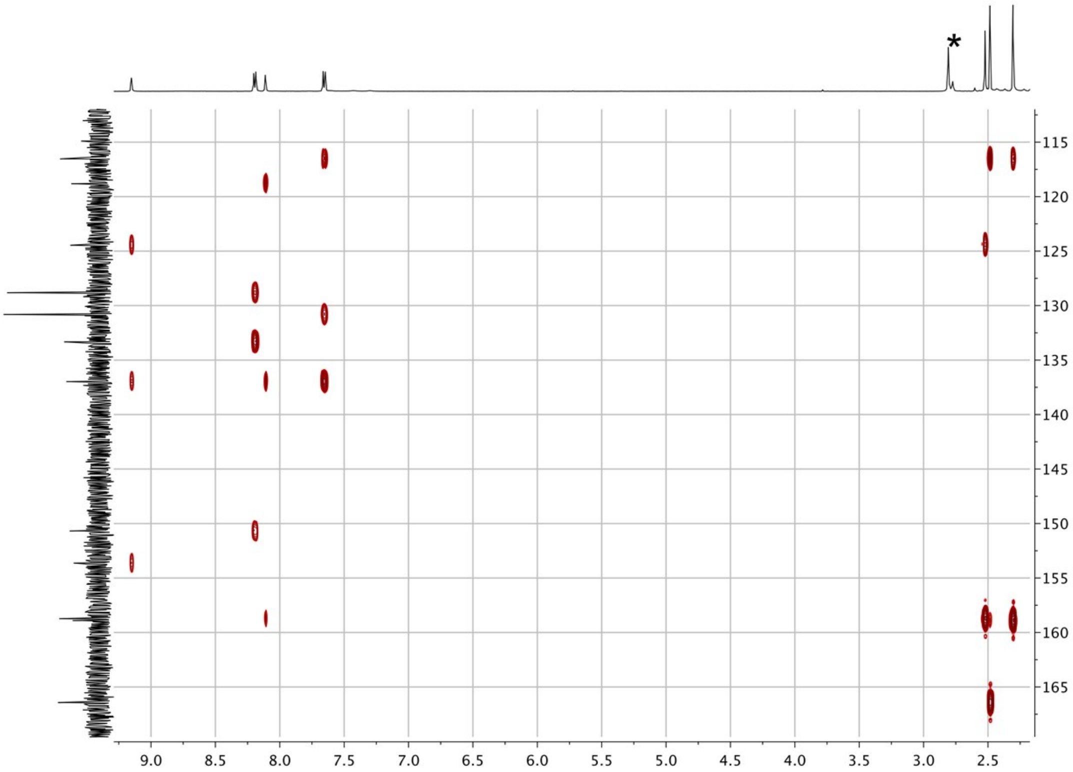

Fig. S28. HMBC (500 MHz ^{1}H, 126 MHz ^{13}C, acetone-d_6, 298 K) spectrum of [Cu(**7**)$_2$][PF$_6$]. * = H_2O, HOD. δ / ppm.

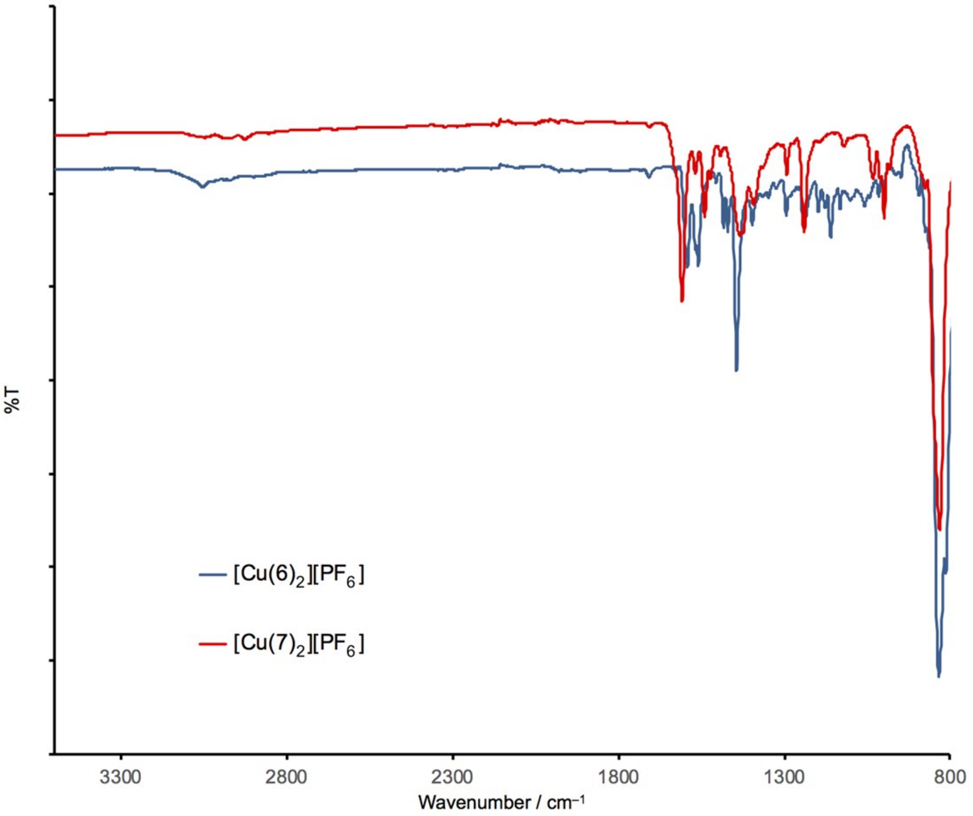

Fig. S29. Solid-state IR spectra of [Cu(**6**)$_2$][PF$_6$] and [Cu(**7**)$_2$][PF$_6$].

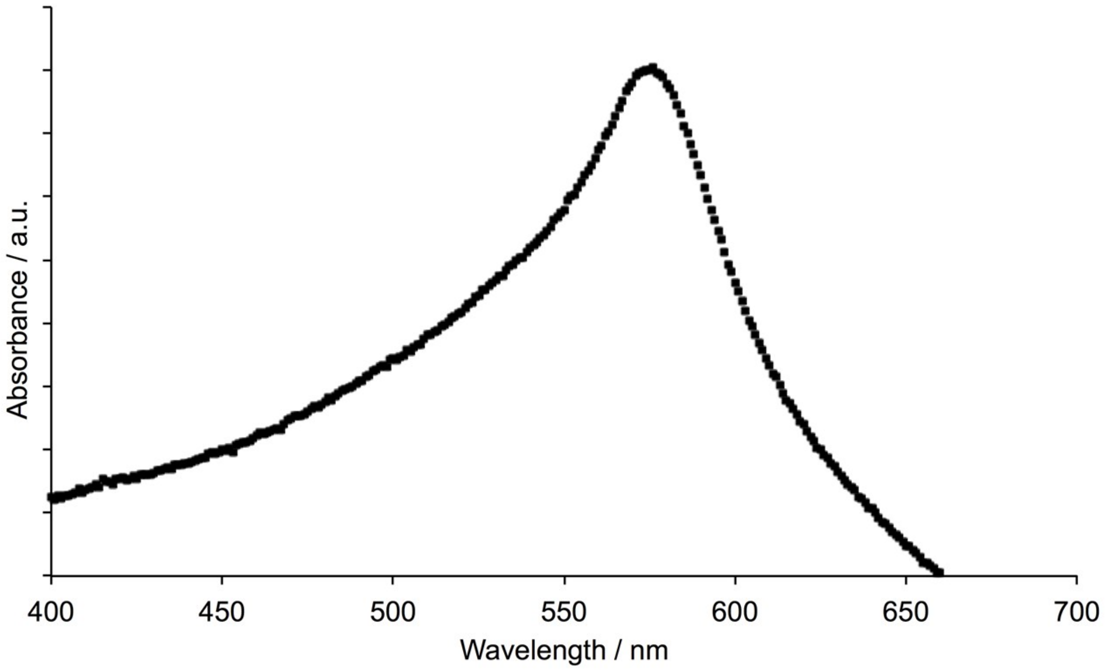

Fig. S30. Solid-state absorption spectrum of NPs functionalized with **3** (following Procedure B in the Experimental Section) after treatment with $[Fe(\mathbf{8})_2][PF_6]_2$.